Surface Winds At Near Shore (SWANS) OSTST project (2017-2020)

Frédéric Frappart (LEGOS, France); **Boris Dewitte** (LEGOS, France); **Orlando Astudillo** (CEAZA, Chile); **Abderrahim Bentamy** (IFREMER, France); **Katerina Goubanova** (CEAZA, Chile); **Marc Mallet** (CNRM, France)

SWANS (2017-2020)

Goals:

- **Estimate wind stress components of the altimeter-derived wind speed**
- **Estimate latent (evaporation) and sensible heat flux along the altimeter tracks in coastal areas combining satellite SST and specific air humidity and altimetric wind speed using the bulk formula**
- **Perform process-oriented studies based on the experimentation with regional oceanic and atmospheric models to better understand the role of air-sea interactions in shaping the low-level atmospheric circulation**

SWANS (2017-2020)

Study area:

- **Humboldt Eastern Boundary Upwelling System (Chile – Peru)**

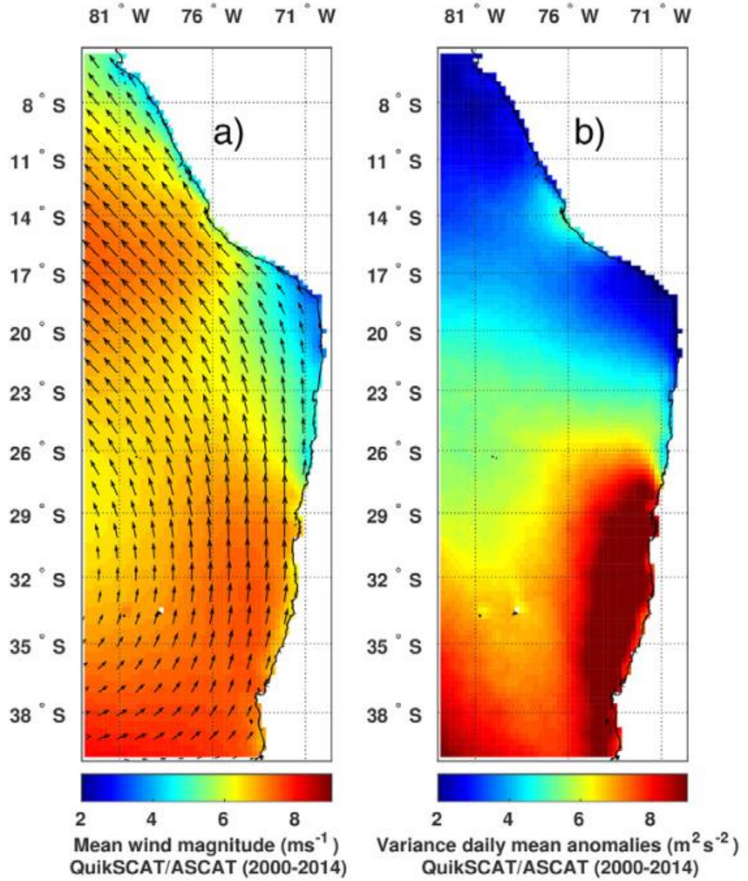

Fig. 4. (a) Mean surface wind speed and wind vectors. (b) Variance of daily intraseasonal anomalies. Intraseasonal anomalies are defined as departures from the monthly means (Lin et al., 2000). Data are from the gridded daily averages QuikSCAT-ASCAT (2000–2014).

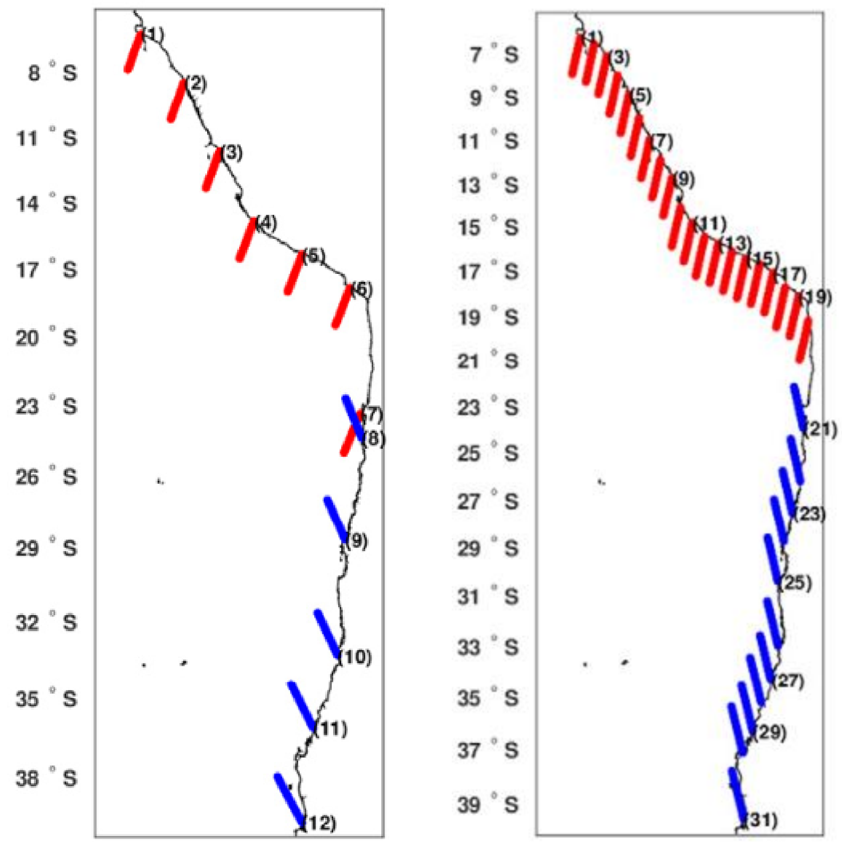

10-day 35-day

repeat orbit tracks

SWANS (2017-2020)

Method:

- **Calibration:**

$$U_{10}^{c} = U_{10} \times slope + offset$$

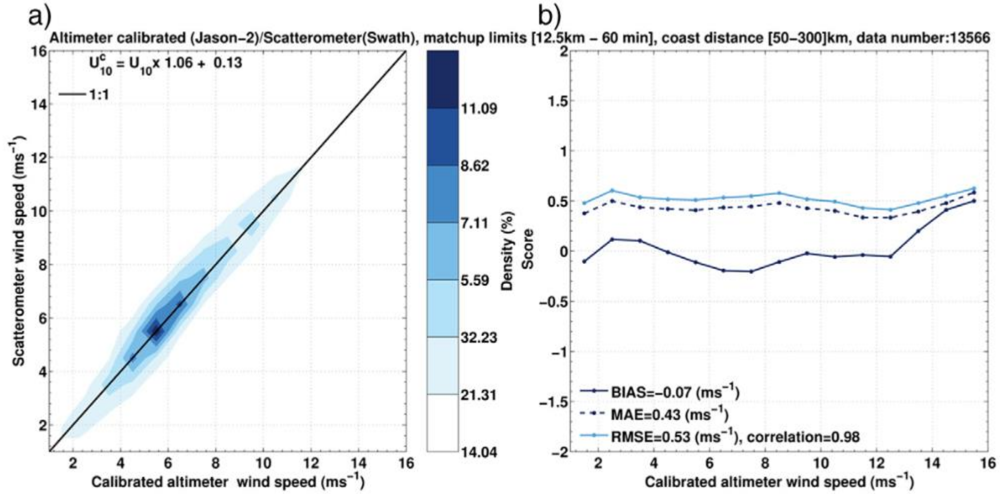

Fig. 3. Calibration result for Jason-2: (a) scatter density plot (shading), (b) mean bias, MAE, RMSE as function of the magnitude of the wind speed (divided in 16 bins). The correlation between the calibrated winds derived from Jason-2 and the swath scatterometer data is provided in panel (b). Statistics are obtained outside the coastal area (50–300 km offshore).

- **Wind stress and drop-off**

$$\tau = \rho_a \times C_d \times \left(U_{10}^{c}\right)^2$$

$$U_x = \cos(\theta - \phi) * U_{10}^{c};\ U_y = \sin(\theta - \phi) * U_{10}^{c}$$

$$\tau x = \cos(\theta - \phi) * \tau;\ \tau y = \sin(\theta - \phi) * \tau$$

$$DO_I(lat) = 100 * \left[\frac{\left(\int_{L_d}^{0} U_{10}^{c}(x, lat)dx - \int_{L_d}^{0} y(x)dx\right)}{\int_{L_d}^{0} y(x)dx}\right]$$

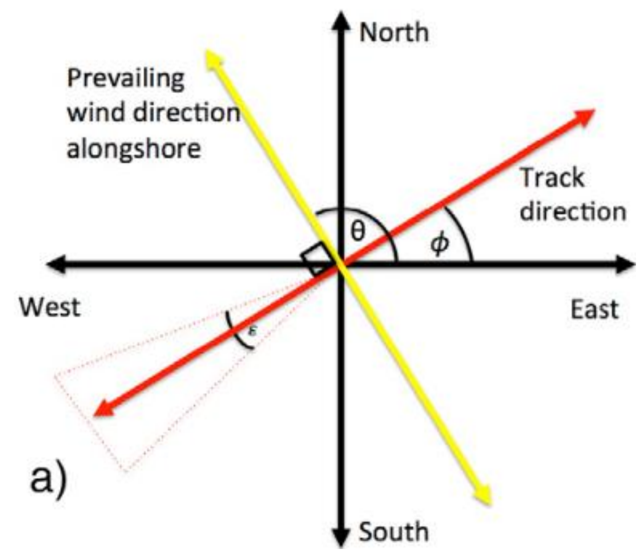

- **Transport and upwelling**

$$\boldsymbol{W} = \frac{1}{\rho_w f} \nabla \times \tau \qquad \boldsymbol{M} = \frac{1}{\rho_w f} \tau \times \boldsymbol{\kappa}$$

SWANS (2017-2020)

Wind speed and drop-off (Astudillo et al., 2017):

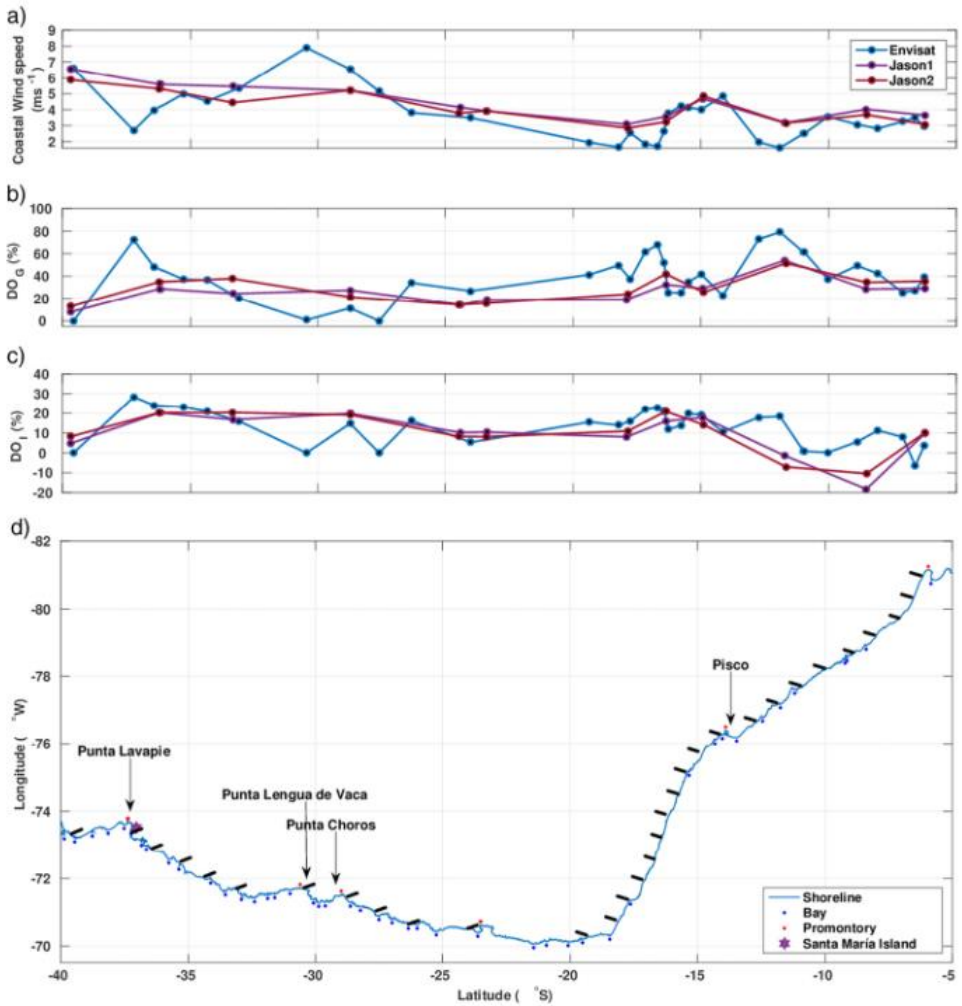

Fig. 7. (a) Coastal wind estimated as the average of the wind speed within the first 10 km off the coast. (b) Wind drop-off index (DO_G). (c) Drop-off shape index (DO_I). (d) Meandering index estimated performing a peak analysis to the coastal longitude. Red circles correspond to the main promontories whereas blue circles indicate the main bays. The black segments correspond to the ENVISAT tracks. Black arrows indicate the location of the main promontories at Punta Lavapie, Punta Lengua de Vaca, Punta Choros and Pisco.

Astudillo, O., Dewitte, B., Mallet, M., Frappart, F., Rutllant, J. A., Ramos, M., Bravo, L., Goubanova, K., & Illig, S. (2017). Surface winds off Peru-Chile: Observing closer to the coast from radar altimetry. *Remote Sensing of Environment*, *191*, 179-196.

SWANS (2017-2020)

Ekman pumping and transport (Astudillo et al., 2017):

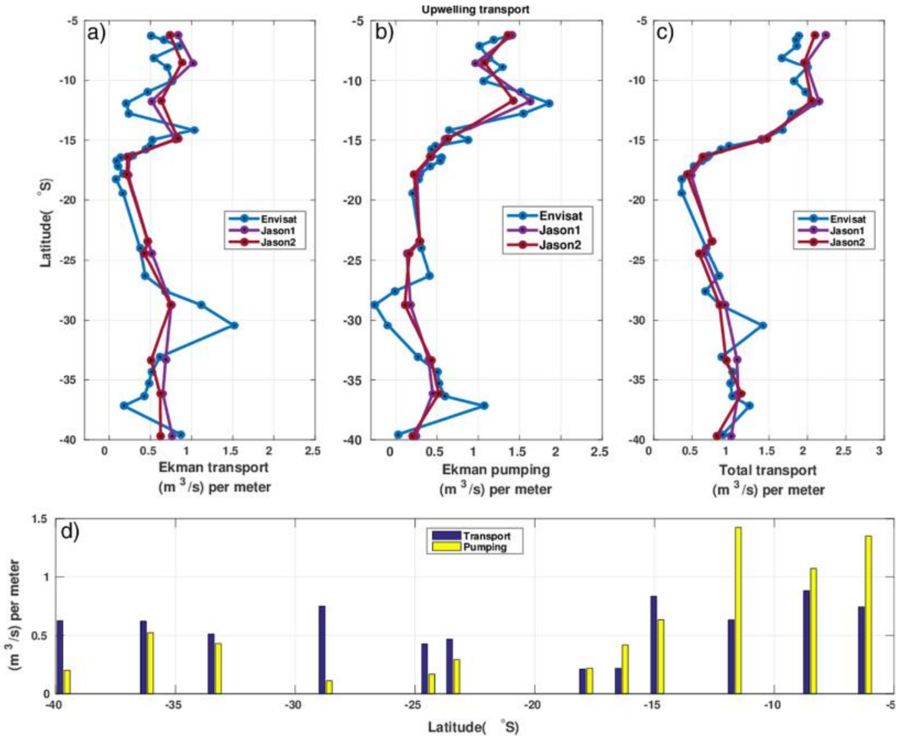

Fig. 8. Contribution of the Ekman transport (a) and Ekman pumping (b) to the mean vertical transport near the coast (within 150 km offshore). (c) Total transport (Ekman transport + Ekman pumping). (d) Comparative detail with the Jason-2 vertical transport associated with Ekman transport and Ekman pumping.

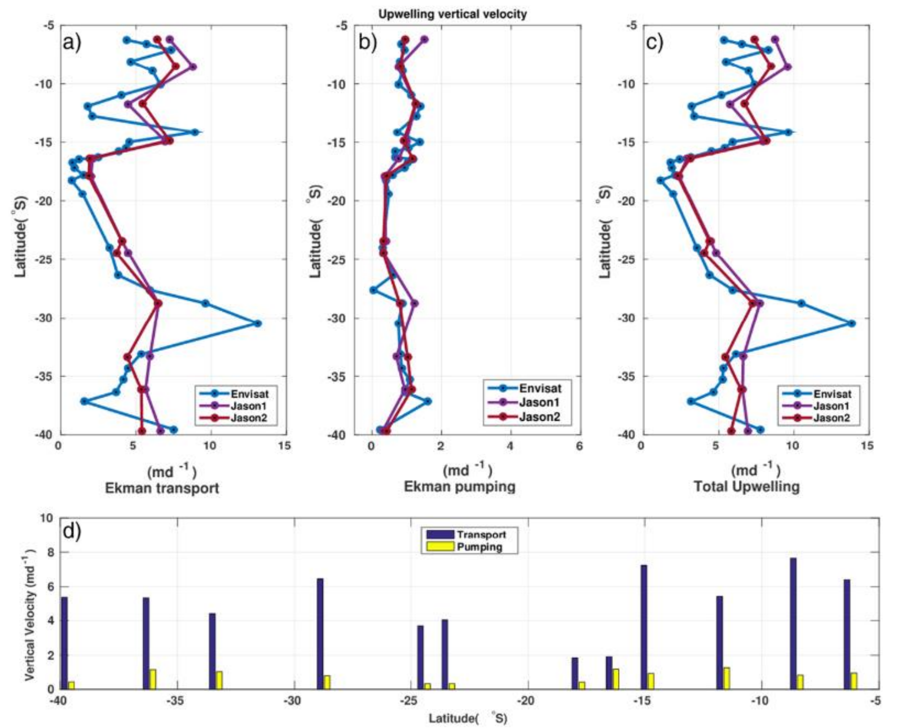

Fig. 9. Mean vertical velocities in the nearshore upwelling zone from (a) Ekman transport, (b) Ekman Pumping and (c) total upwelling (Ekman transport + Ekman pumping). (Comparative detail with the Jason-2 vertical velocities contributions induced by Ekman transport and Ekman pumping.

SWANS (2017-2020)

Sensitivity of the oceanic circulation to coastal wind profiles in a high-resolution model

- **Model**: CROCO at 3km resolution (1/36°)
- **Domain** : central Chile
- **Experiments**: forced simulations (15-years, permanent year 2005) with and without including a coastal wind profiles in the atmospheric forcing
- **Method**: heat budget analysis
- **Objective**: Does the consideration of a wind-drop off in the atmospheric forcing reduces the cool biais?
- **Answer**: Yes but not for the reason we thought

SWANS (2017-2020)

Heat budget analysis in a 50-km coastal fringe:

Simulation without drop-off | **Simulation with drop-off**

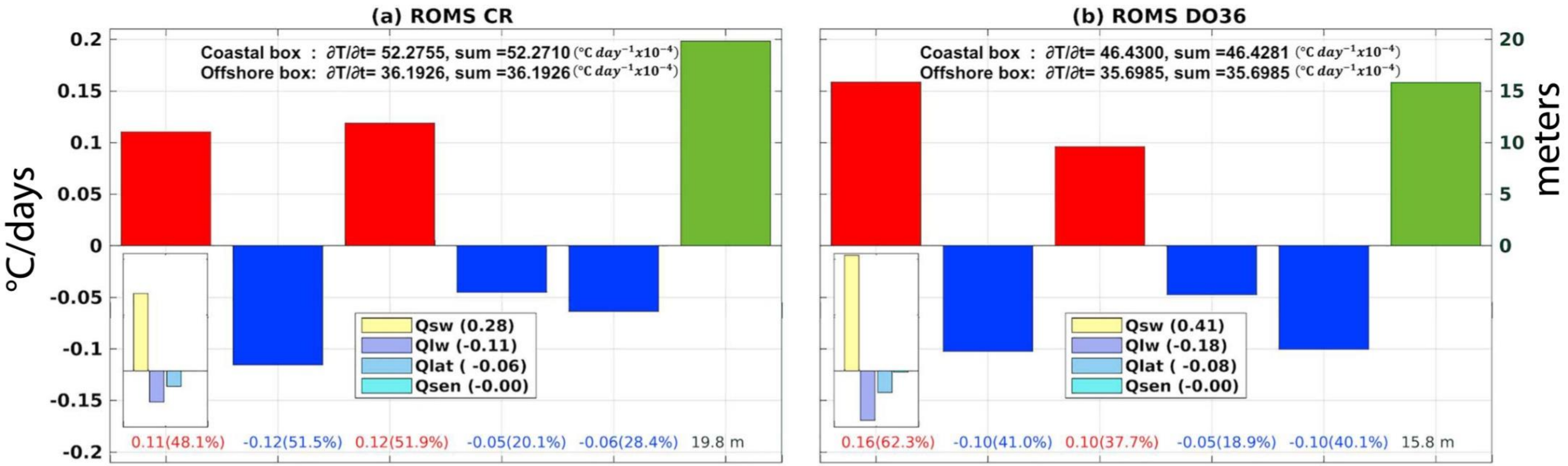

$\frac{Q_{net}}{\rho C_p H_{mix}}$ $\quad -u\frac{\partial T}{\partial x}$ $\quad -v\frac{\partial T}{\partial y}$ $\quad -w\frac{\partial T}{\partial z}$ $\quad -\frac{\partial}{\partial z}\left[K_z\frac{\partial T}{\partial z}\right]$ $\quad H_{mix}$ $\qquad \frac{Q_{net}}{\rho C_p H_{mix}}$ $\quad -u\frac{\partial T}{\partial x}$ $\quad -v\frac{\partial T}{\partial y}$ $\quad -w\frac{\partial T}{\partial z}$ $\quad -\frac{\partial}{\partial z}\left[K_z\frac{\partial T}{\partial z}\right]$ $\quad H_{mix}$

Astudillo, O., Dewitte, B., Mallet, M., Rutllant, J. A., Goubanova, K., Frappart, F., et al (2019). Sensitivity of the near-shore oceanic circulation off Central Chile to coastal wind profiles characteristics. *Journal of Geophysical Research: Oceans*, 124, 4644– 4676.

SWANS (2017-2020)

Results (Astudillo et al., 2019):

•The presence of a wind drop-off reduces Ekman transport with is partially compensated by an increase an Ekman pumping. On the other hand, it yields a reduction in vertical mixing (shallower mixed-layer) which increase the warming tendency associated to heat fluxes (Solar radiation is more efficient in warming SST).

• In addition, the coastal wind profiles impact the baroclinic instability of the coastal currents, which modulates the off-shore eddy flux: Costal winds are thus influential on the regional oceanic circulation.

• Coastal wind profiles are not realistic in atmospheric Reanalyses (even the state-of-the art), which explains why oceanic Reanalyses have a persistent bias in mean EKE along the coast of Peru/Chile.

SWANS (2017-2020)

Modulation of mean EKE at ENSO timescales:

Mean EKE changes are associated to the modulation of the baroclinic instability of the coastal currents due to the oceanic teleconnection (ENSO) and to wind work associated to along-shore wind changes during ENSO.

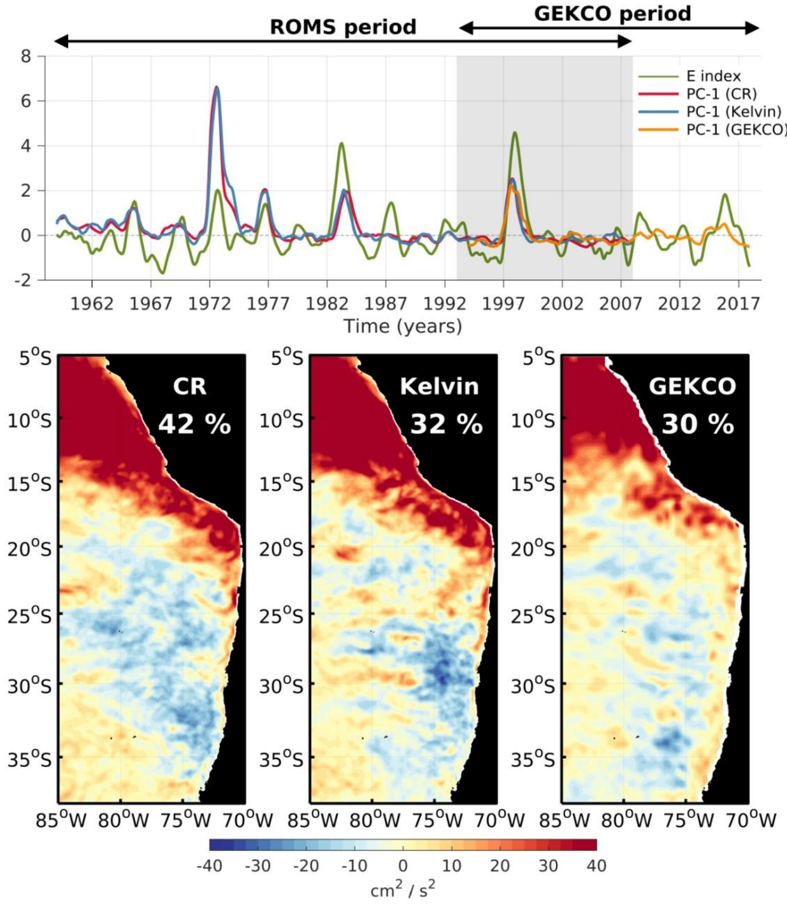

Conejero C., B. Dewitte, V. Garçon, J. Sudre and I. Montes (in press): ENSO diversity driving low-frequency change in mesoscale activity off Peru and Chile, Nature Scientific Report.

SWANS (2017-2020)

Perspective:

- **Document long-term trends in coastal wind profiles and compare with long-term trend in costal sea level/SST: Can observed discrepancies between sea level trends in the coastal zone and the open-ocean can be explained by trends in the wind stress curl along the coast?**
- **Enhance the network of meteorological stations in collaboration with partners (Peru/Chile): i.e. maintain stations in location of satellite track for Cal/Val purpose (on-going with CEAZA (Chile))**
- **Test correction of coastal winds in atmospheric Reanalysis for improving oceanic reanalysis products (collaboration with Mercator-ocean)**
- **Link with on-going project UPWESWIND: Use of HR Sentinel-1A SAR images to complement Scatterometer/Radiometer products in the coastal zone. HR merged products (0.125°, 1h) on the 2000-2019 period => Indirect «validation» with ocean modeling (SWANS for Humboldt and California EBUS)**